

Performance Analysis of Single-carrier Overlap FDE

Tatsunori OBARA[†] Kazuki TAKEDA[†] and Fumiyuki ADACHI[‡]

Dept. of Electrical and Communication Engineering, Graduate School of Engineering, Tohoku University
6-6-05, Aza-Aoba, Aramaki, Aoba-ku, Sendai, 980-8579, JAPAN
E-mail: [†]{obara, kazuki}@mobile.ecei.tohoku.ac.jp [‡]adachi@ecei.tohoku.ac.jp

Abstract— In the single-carrier (SC) transmission, minimum mean square error frequency-domain equalization (MMSE-FDE) can achieve a good bit error rate (BER) performance in a frequency-selective fading channel. The conventional FDE requires the insertion of cyclic prefix (CP) to make the received signal block to be a circular convolution of the transmit signal and the channel. Overlap FDE requires no CP insertion. However, its BER performance improvement is limited by the residual inter-block interference (IBI). In this paper, we present the theoretical analysis of the BER performance achievable with overlap FDE by taking into account the residual IBI after overlap FDE. Then, by using the Gaussian approximation of the residual IBI as well as the residual inter-symbol interference (ISI), we derive the conditional BER for the given set of the channel gains. The average BER performance is numerically evaluated.

Keywords; Frequency-selective fading channel, overlap FDE, single-carrier transmission

I. INTRODUCTION

The broadband wireless channel is composed of many propagation paths with different time delays and produces strong inter-symbol interference (ISI) in the broadband single-carrier (SC) transmission [1], [2]. The use of minimum mean square error frequency-domain equalization (MMSE-FDE) can take advantage of the channel frequency-selectivity and achieve a good bit error rate (BER) performance [3]-[5]. The conventional FDE requires the insertion of cyclic prefix (CP) to make the received signal block to be a circular convolution of the transmit signal block and the channel. The CP insertion reduces the transmission throughput. Furthermore, when the maximum time delay of the channel exceeds the CP length, the BER performance degrades due to the residual inter-block interference (IBI) after FDE.

Overlap FDE requires no CP insertion, but its BER performance improvement is limited by the residual IBI after FDE [6], [7]. It was shown that overlap FDE provides higher throughput than the conventional FDE at the cost of increased complexity [8]. The theoretical analysis of overlap FDE for the multi-carrier (MC) transmission was presented in [9]. In this paper, we present the theoretical analysis of the BER performance achievable with overlap FDE for the SC transmission by taking into account the residual IBI after MMSE-FDE. Then, by using the Gaussian approximation of the residual IBI, we derive the conditional BER for the given set of the channel gains. The average BER performance is numerically evaluated.

The remainder of this paper is organized as follows. Section II describes overlap FDE. The system model of the SC

transmission using overlap FDE is presented in Sect. III. In Sect. IV, we present the theoretical BER analysis. The theoretical BER performance is numerically evaluated in Sect. V. Section VI offers some conclusions.

II. OVERLAP FDE [6]-[8]

The residual IBI after MMSE-FDE is a circular convolution of the IBI and the impulse response of MMSE-FDE filter. Figure 1 shows the impulse response of the MMSE-FDE filter for an $L=16$ -path Rayleigh fading channel with uniform power delay profile when the block size of fast Fourier transform (FFT) is $N_c=256$. As seen from Fig. 1, the MMSE-FDE filter impulse response concentrates at a vicinity of time $t=0$. Therefore, the residual IBI is localized only near the both ends of the N_c -symbol block after MMSE-FDE. The overlap FDE is based on this observation. At the receiver, the received symbol sequence is divided into a sequence of M -symbol blocks ($M \leq N_c$). Then, N_c -point FFT is applied to an N_c -symbol block centering the M -symbol block of interest. After MMSE-FDE, the central M -symbol block in the equalized N_c -symbol block is picked up to suppress the residual IBI. The FFT intervals for consecutive M -symbol blocks overlap as shown in Fig. 2.

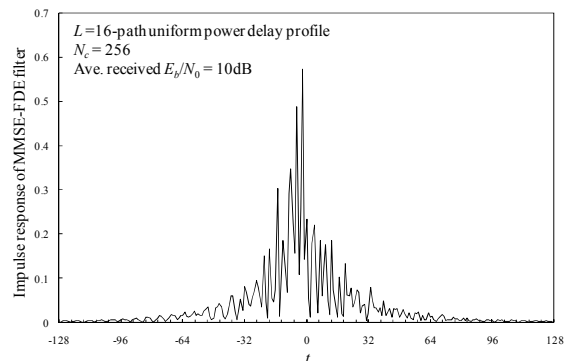


Fig. 1 Impulse response of MMSE-FDE filter.

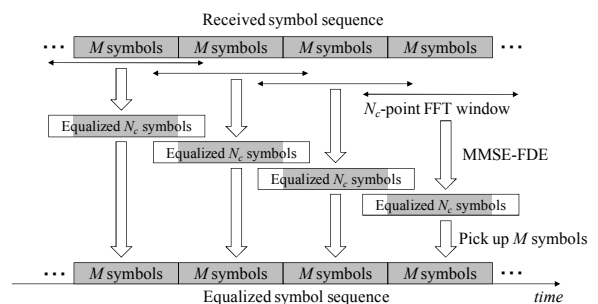


Fig. 2 Block signal processing of overlap FDE.

III. SYSTEM MODEL

A. Signal representation

Figure 3 illustrates the transmitter and receiver structure for the SC transmission using overlap FDE. In this paper, a symbol-spaced discrete-time representation is used. At the transmitter, the binary information sequence is data-modulated, and then the data-modulated symbol sequence $\{s(t); t = \dots, -1, 0, 1, \dots\}$ is transmitted without CP insertion. The transmitted symbol sequence $\{s(t); t = \dots, -1, 0, 1, \dots\}$ is received via a frequency-selective fading channel. In this paper, we assume a sample-spaced L -path frequency-selective block fading channel. The channel impulse response can be expressed as

$$h(\tau) = \sum_{l=0}^{L-1} h_l \delta(\tau - \tau_l), \quad (1)$$

where h_l and τ_l are the complex-valued path gain and the delay time of the l th path, respectively, with $\sum_{l=0}^{L-1} E[|h_l|^2] = 1$ ($E[\cdot]$ denotes the ensemble average operation).

The received N_c -symbol block $\{r(t); t=0 \sim N_c-1\}$ can be expressed as

$$r(t) = \sqrt{\frac{2E_s}{T_s}} \sum_{l=0}^{L-1} h_l s((t - \tau_l) \bmod N_c) + v(t) + \eta(t), \quad (2)$$

where E_s and T_s are the symbol energy and the symbol duration, respectively. $v(t)$ and $\eta(t)$ are the IBI component and the additive white Gaussian noise (AWGN) with zero mean and variance $2N_0/T_s$ with N_0 being the single-sided power spectrum density, respectively. $v(t)$ is given as

$$v(t) = \sqrt{\frac{2E_s}{T_s}} \sum_{l=0}^{L-1} h_l \{s(t - \tau_l) - s((t - \tau_l) \bmod N_c)\} \times \{u(t) - u(t - \tau_l)\} \quad (3)$$

where $u(t)$ is the unit step function.

B. Overlap FDE

The received N_c -symbol block $\{r(t); t=0 \sim N_c-1\}$ is transformed by an N_c -point FFT into the frequency-domain signal $\{R(k); k=0 \sim N_c-1\}$. $R(k)$ can be expressed as

$$R(k) = \sum_{t=0}^{N_c-1} r(t) \exp\left(-j2\pi k \frac{t}{N_c}\right) = \sqrt{\frac{2E_s}{T_s}} H(k) S(k) + N(k) + \Pi(k) \quad (4)$$

where $H(k)$ is the channel gain at the k th frequency, and $S(k)$, $N(k)$, and $\Pi(k)$ are the signal component, the IBI component, and the noise component, respectively, given as

$$\begin{cases} H(k) = \sum_{l=0}^{L-1} h_l \exp\left(-j2\pi k \frac{\tau_l}{N_c}\right) \\ S(k) = \sum_{t=0}^{N_c-1} s(t) \exp\left(-j2\pi k \frac{t}{N_c}\right) \\ N(k) = \sum_{t=0}^{N_c-1} v(t) \exp\left(-j2\pi k \frac{t}{N_c}\right) \\ \Pi(k) = \sum_{t=0}^{N_c-1} \eta(t) \exp\left(-j2\pi k \frac{t}{N_c}\right) \end{cases} \quad (5)$$

Then, the frequency-domain signal $R(k)$ is multiplied by the MMSE-FDE weight $W(k)$ as

$$\hat{R}(k) = R(k)W(k) = \sqrt{\frac{2E_s}{T_s}} \hat{H}(k) S(k) + \hat{N}(k) + \hat{\Pi}(k), \quad (6)$$

where $\hat{H}(k)$, $\hat{N}(k)$, and $\hat{\Pi}(k)$ are the equivalent channel gain, the IBI component, and the noise component after the MMSE-FDE, respectively, given as

$$\begin{cases} \hat{H}(k) = H(k)W(k) \\ \hat{N}(k) = N(k)W(k) \\ \hat{\Pi}(k) = \Pi(k)W(k) \end{cases} \quad (7)$$

The MMSE-FDE weight $W(k)$ is given as [8]

$$W(k) = \frac{H^*(k)}{|H(k)|^2 + \Lambda^{-1}}, \quad (8)$$

where Λ denotes the signal-to-interference plus noise power ratio (SINR) given as

$$\Lambda^{-1} = \frac{2}{N_c} \sum_{l=0}^{L-1} |h_l|^2 \tau_l + \left(\frac{E_s}{N_0}\right)^{-1}. \quad (9)$$

The frequency-domain signal $\{\hat{R}(k); k=0 \sim N_c-1\}$ is transformed by an N_c -point inverse FFT (IFFT) back to the time-domain signal $\{\hat{r}(t); t=0 \sim N_c-1\}$ as

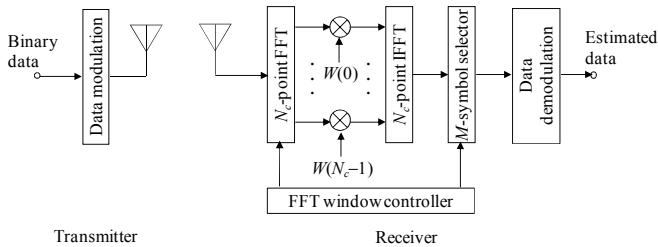


Fig. 3 Model of SC transmission using overlap FDE.

$$\begin{aligned}\hat{r}(t) &= \frac{1}{N_c} \sum_{k=0}^{N_c-1} \hat{R}(k) \exp\left(j2\pi t \frac{k}{N_c}\right) \\ &= \sqrt{\frac{2E_s}{T_s}} \left\{ \frac{1}{N_c} \sum_{k=0}^{N_c-1} \hat{H}(k) \right\} s(t) + \mu(t) + \hat{v}(t) + \hat{\eta}(t)\end{aligned}\quad (10)$$

where $\mu(t)$, $\hat{v}(t)$, and $\hat{\eta}(t)$ are the residual inter-symbol interference (ISI), the residual IBI, and the noise component, respectively, given as

$$\begin{cases} \mu(t) = \frac{1}{N_c} \sqrt{\frac{2E_s}{T_s}} \sum_{k=0}^{N_c-1} \hat{H}(k) \sum_{\substack{t'=0 \\ \neq t}}^{N_c-1} s(t') \exp\left(j2\pi k \frac{t-t'}{N_c}\right) \\ \hat{v}(t) = \frac{1}{N_c} \sum_{k=0}^{N_c-1} \hat{N}(k) \exp\left(j2\pi t \frac{k}{N_c}\right) \\ \hat{\eta}(t) = \frac{1}{N_c} \sum_{k=0}^{N_c-1} \hat{\Pi}(k) \exp\left(j2\pi t \frac{k}{N_c}\right) \end{cases}\quad (11)$$

Only the central M -symbol block is picked up from the equalized N_c -symbol block. To suppress the residual IBI sufficiently, M should be much smaller than N_c .

IV. BER ANALYSIS

It can be understood from Eq. (10) that $\hat{r}(t)$ at time t is a complex-valued random variable with mean $(2E_s/T_s)(1/N_c) \sum_{k=0}^{N_c-1} \hat{H}(k) s(t)$. By approximating $\mu(t)$ and $\hat{v}(t)$ respectively as a zero-mean complex-valued Gaussian variable, the sum of the residual ISI, residual IBI, and noise, $\psi(t) = \mu(t) + \hat{v}(t) + \hat{\eta}(t)$, can be treated as a new zero-mean complex-valued Gaussian variable. The variance $2\sigma_\psi^2(t)$ of $\psi(t)$ is given as

$$2\sigma_\psi^2(t) = E[|\psi(t)|^2] = 2\sigma_\mu^2(t) + 2\sigma_v^2(t) + 2\sigma_\eta^2(t), \quad (12)$$

where $2\sigma_\mu^2(t)$, $2\sigma_v^2(t)$, and $2\sigma_\eta^2(t)$ are the variances of $\mu(t)$, $\hat{v}(t)$, and $\hat{\eta}(t)$, respectively. $\sigma_\mu^2(t)$ and $\sigma_\eta^2(t)$ are given as [10]

$$\begin{cases} \sigma_\mu^2(t) = \frac{1}{2} E[|\mu(t)|^2] \\ = \frac{E_s}{T_s} \left(\frac{1}{N_c} \sum_{k=0}^{N_c-1} |\hat{H}(k)|^2 - \left| \frac{1}{N_c} \sum_{k=0}^{N_c-1} \hat{H}(k) \right|^2 \right) \\ \sigma_\eta^2(t) = \frac{1}{2} E[|\hat{\eta}(t)|^2] \\ = \frac{N_0}{T_s} \frac{1}{N_c} \sum_{k=0}^{N_c-1} |W(k)|^2 \end{cases}\quad (13)$$

The residual IBI power $\sigma_v^2(t)$ can be derived as (for the sake of brevity, the derivation is omitted)

$$\begin{aligned}\sigma_v^2(t) &= \frac{1}{2} E[|\hat{v}(t)|^2] \\ &= \frac{2E_s}{T_s} \sum_{l=0}^{L-1} |h_l|^2 \sum_{\tau=0}^{\tau_l-1} |w(t-\tau_l)|^2\end{aligned}\quad (14)$$

where $w(t)$ is the impulse response of the MMSE-FDE filter given as

$$w(t) = \frac{1}{N_c} \sum_{k=0}^{N_c-1} W(k) \exp\left(j2\pi t \frac{k}{N_c}\right).\quad (15)$$

It can be understood from Eq. (14) that $\sigma_v^2(t)$ is a function of the symbol index t , while $\sigma_\mu^2(t)$ and $\sigma_\eta^2(t)$ are not.

Assuming QPSK data-modulation, the conditional BER for the given channel realization $\mathbf{H}=[H(0), \dots, H(N_c-1)]$ at the t th symbol position can be given as [2]

$$p_e\left(\frac{E_s}{N_0}, t, \mathbf{H}\right) = \frac{1}{2} \operatorname{erfc}\left[\sqrt{\frac{1}{4} \gamma\left(\frac{E_s}{N_0}, t, \mathbf{H}\right)}\right], \quad (16)$$

where $\operatorname{erfc}(x) = (2/\sqrt{\pi}) \int_x^\infty \exp(-u^2) du$ is the complementary error function and $\gamma(E_s/N_0, t, \mathbf{H})$ is the conditional SINR given as

$$\begin{aligned}\gamma\left(\frac{E_s}{N_0}, t, \mathbf{H}\right) &= \frac{\left| \sqrt{\frac{2E_s}{T_s}} \frac{1}{N_c} \sum_{k=0}^{N_c-1} \hat{H}(k) \right|^2}{\sigma_\psi^2(t)} \\ &= \frac{2 \frac{E_s}{N_0} \left| \frac{1}{N_c} \sum_{k=0}^{N_c-1} \hat{H}(k) \right|^2}{\frac{E_s}{N_0} \left(\frac{1}{N_c} \sum_{k=0}^{N_c-1} |\hat{H}(k)|^2 - \left| \frac{1}{N_c} \sum_{k=0}^{N_c-1} \hat{H}(k) \right|^2 \right)} \\ &\quad + 2 \frac{E_s}{N_0} \sum_{l=0}^{L-1} |h_l|^2 \sum_{\tau=0}^{\tau_l-1} |w(t-\tau_l)|^2 \\ &\quad + \frac{1}{N_c} \sum_{k=0}^{N_c-1} |W(k)|^2\end{aligned}\quad (17)$$

In overlap FDE, only the central M -symbol block $\{\hat{r}(t); t = (N_c - M)/2 \sim (N_c + M)/2 - 1\}$ is picked up from the equalized N_c -symbol block. The average BER over the M -symbol block can be expressed as

$$p_b\left(\frac{E_s}{N_0}, M, \mathbf{H}\right) = \frac{1}{M} \sum_{m=0}^{M-1} p_e\left(\frac{E_s}{N_0}, m + \frac{N_c - M}{2}, \mathbf{H}\right).\quad (18)$$

The average BER of the SC transmission using overlap FDE can be numerically evaluated by averaging Eq. (18) over all possible \mathbf{H} as

$$P_b\left(\frac{E_s}{N_0}, M\right) = \operatorname{ave}_{\text{all } \mathbf{H}} p_b\left(\frac{E_s}{N_0}, M, \mathbf{H}\right).\quad (19)$$

V. NUMERICAL COMPUTATION AND COMPUTER SIMULATION

The theoretical BER performance is numerically evaluated using Monte-Carlo numerical computation method and compared with the simulation results. Table 1 summarizes the numerical and simulation conditions. We assume QPSK data-modulation. The propagation channel is assumed to be a frequency-selective block Rayleigh fading channel having a symbol-spaced $L=16$ -path exponential power delay profile with decay factor α . The ideal channel estimation is assumed.

Table 1 Numerical and simulation conditions

Data modulation	QPSK	
FFT/IFFT block length	$N_c=256$	
Channel model	Frequency-selective block Rayleigh fading	
	Power delay profile	$L=16$ -path exponential
	Decay factor	$\alpha=0, 6\text{dB}$
	Delay time	$\tau_l=l$
Channel estimation	Ideal	

A. Residual IBI power distribution

Figure 4 shows the distribution of the average residual IBI power normalized by the signal power $P=E_s/T_s$ within the equalized N_c -symbol block as a function of the symbol index t for $\alpha=0\text{dB}$. Theoretical and simulated results agree fairly well and this confirms the validity of our theoretical analysis. As seen from Fig. 4, the residual IBI power is small in the central part of N_c -symbol block. Therefore, by picking up only the central part from the equalized N_c -symbol block, the residual IBI can be better suppressed.

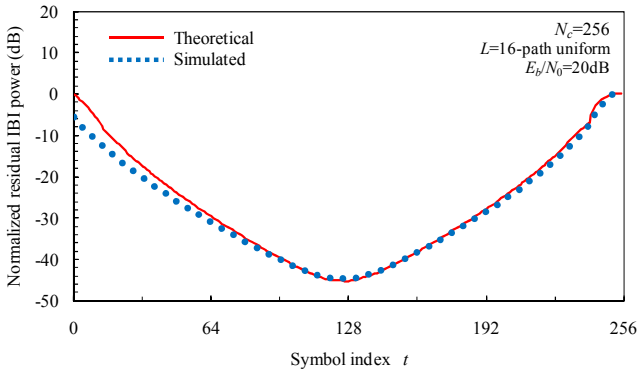
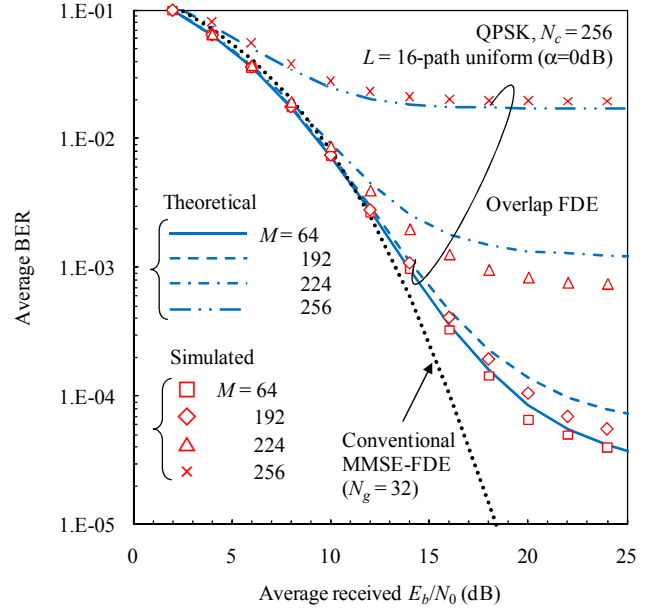
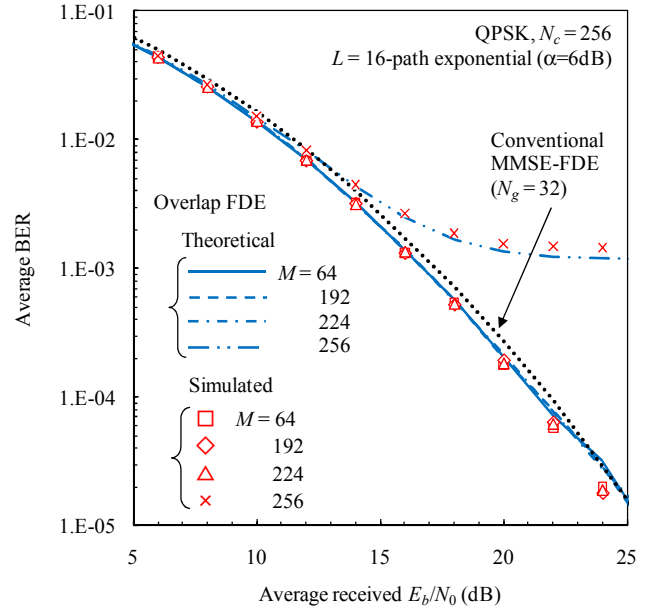


Fig. 4 Residual IBI power distribution within N_c -symbol block.



(a) $\alpha=0\text{dB}$



(b) $\alpha=6\text{dB}$

Fig. 5 Average BER performance.

B. Average BER performance

Figure 5 plots the average BER performance of the SC transmission using overlap FDE as a function of the average received bit energy-to-noise power spectrum density ratio E_b/N_0 ($=0.5E_s/N_0$). For comparison, the BER performance of the SC transmission using the conventional MMSE-FDE is also plotted, where the CP length is assumed to be $N_g=32$ symbols and the E_b/N_0 loss due to the CP insertion is taken into account. Figure 5(a) plots the BER performance for $\alpha=0\text{dB}$. It

is seen from Fig. 5(a) that as M becomes smaller, the BER performance of overlap FDE approaches that of the conventional MMSE-FDE. However, since overlap FDE cannot perfectly suppress the residual IBI after MMSE-FDE, the BER performance degrades in high E_b/N_0 regions. Figure 5(b) plots the BER performance for $\alpha=6\text{dB}$. As shown in Fig. 5(b), when $\alpha=6\text{dB}$, overlap FDE can achieve almost the same BER performance as the conventional MMSE-FDE except for $M=N_c$. This is because when $\alpha=6\text{dB}$, the channel frequency-selectivity becomes weaker and therefore, the residual IBI after MMSE-FDE becomes smaller in M -chip block. It can be understood from Fig. 5(b) that when $\alpha=6\text{dB}$, $M=224$ is sufficient to suppress the residual IBI. In Fig. 5, a fairly good agreement between the theoretical and simulation results is seen.

VI. CONCLUSION

In this paper, we presented the theoretical BER analysis of the SC transmission using overlap FDE which requires no CP insertion. Overlap FDE can suppress the residual IBI after FDE by picking up only the central M -symbol block from the equalized N_c -symbol block. The conditional BER for the given set of the channel gain was derived and was confirmed by the computer simulation. It was shown that as M becomes smaller, the BER performance of overlap FDE approaches that of the conventional MMSE-FDE; however, in high E_b/N_0 regions, the BER performance of overlap FDE degrades due to the residual IBI. When the channel frequency-selectivity is weak, the residual IBI becomes smaller and therefore, overlap FDE can

achieve almost the same BER performance as the conventional MMSE-FDE.

REFERENCES

- [1] W.C., Jakes Jr, Ed, *Microwave mobile communications*, Wiley, Newyork, 1974.
- [2] J.G. Proakis, *Digital communications*, 4th ed., McGraw-Hill, 2001.
- [3] D. Falconer, S. L. Ariyavisitakul, A. Benyamin-Seeyar, and B. Eidson, "Frequency domain equalization for single-carrier broadband wireless systems," *IEEE Commun.*, Vol. 40, No.4, pp 58-66, Apr. 2002.
- [4] M. V. Clark, "Adaptive frequency-domain equalization and diversity combining for broadband wireless communications," *IEEE J. Select. Areas. Commun.*, Vol. 16, No. 8, pp. 1385-1395, Oct.1998.
- [5] F. Adachi, D. Garg, S. Takaoka, and K. Takeda, "Broadband CDMA techniques," *IEEE Wireless Commun.*, Vol. 12, No.2, pp.8-18, Apr. 2005.
- [6] I. Martoyo, T. Weiss, F. Capar, and F. K. Jondral, "Low complexity CDMA downlink receiver based on frequency domain equalization," *IEEE Vehicular Technology Conference (VTC) '03 fall*, Orlando, Florida, USA, Sept. 2003.
- [7] T. Takeda, H. Tomeba, and F. Adachi, "Iterative overlap FDE for DS-CDMA without GI," *IEEE 64th VTC*, Montreal, Quebec, Canada, Sept. 2006.
- [8] Kazuki Takeda, Hiromichi Tomeba, Kazuaki Takeda and Fumiyuki Adachi, "DS-CDMA HARQ with Overlap FDE," *IEICE Trans. Commun.*, Vol. E90-B, No. 11, pp. 3189-3196, Nov. 2007.
- [9] H. Tomeba, K. Takeda, and F. Adachi, "BER Performance Analysis of MC-CDMA with Overlap-FDE," *IEICE Trans. Commun.*, Vol. E91-B, No. 3, pp. 795-804, Mar. 2008.
- [10] F. Adachi and K. Takeda, "Bit error rate analysis of DS-CDMA with joint frequency-domain equalization and antenna diversity combining," *IEICE Trans. Commun.*, Vol. E87-B, No. 10, pp. 2991-3002, Oct. 2004.